

## Suspended AlGaIn/GaN HEMT NO<sub>2</sub> Gas Sensor Integrated with Micro-heater

Sun, Jianwen; Sokolovskij, Robert; Iervolino, Elina; Liu, Zewen; Sarro, Pasqualina M.; Zhang, Guoqi

**DOI**

[10.1109/JMEMS.2019.2943403](https://doi.org/10.1109/JMEMS.2019.2943403)

**Publication date**

2019

**Document Version**

Final published version

**Published in**

Journal of Microelectromechanical Systems

**Citation (APA)**

Sun, J., Sokolovskij, R., Iervolino, E., Liu, Z., Sarro, P. M., & Zhang, G. (2019). Suspended AlGaIn/GaN HEMT NO<sub>2</sub> Gas Sensor Integrated with Micro-heater. *Journal of Microelectromechanical Systems*, 28(6), 997-1004. Article 8856274. <https://doi.org/10.1109/JMEMS.2019.2943403>

**Important note**

To cite this publication, please use the final published version (if applicable). Please check the document version above.

**Copyright**

Other than for strictly personal use, it is not permitted to download, forward or distribute the text or part of it, without the consent of the author(s) and/or copyright holder(s), unless the work is under an open content license such as Creative Commons.

**Takedown policy**

Please contact us and provide details if you believe this document breaches copyrights. We will remove access to the work immediately and investigate your claim.

***Green Open Access added to TU Delft Institutional Repository***

***'You share, we take care!' - Taverne project***

**<https://www.openaccess.nl/en/you-share-we-take-care>**

Otherwise as indicated in the copyright section: the publisher is the copyright holder of this work and the author uses the Dutch legislation to make this work public.

# Suspended AlGaIn/GaN HEMT NO<sub>2</sub> Gas Sensor Integrated With Micro-heater

Jianwen Sun<sup>1</sup>, Robert Sokolovskij, Elina Iervolino, Zewen Liu, Pasqualina M. Sarro, *Fellow, IEEE*, and Guoqi Zhang, *Fellow, IEEE*

**Abstract**—We developed an AlGaIn/GaN high electron mobility transistor (HEMT) sensor with a tungsten trioxide (WO<sub>3</sub>) nano-film modified gate for nitrogen dioxide (NO<sub>2</sub>) detection. The device has a suspended circular membrane structure and an integrated micro-heater. The thermal characteristic of the Platinum (Pt) micro-heater and the HEMT self-heating are studied and modeled. A significant detection is observed for exposure to a low concentration of 100 ppb NO<sub>2</sub>/N<sub>2</sub> at ~300 °C. For a 1 ppm NO<sub>2</sub> gas, a high sensitivity of 1.1% with a response (recovery) time of 88 second (132 second) is obtained. The effects of relative humidity and temperature on the gas sensor response properties in air are also studied. Based on the excellent sensing performance and inherent advantages of low power consumption, the investigated sensor provides a viable alternative high performance NO<sub>2</sub> sensing applications. It is suitable for continuous environmental monitoring system or high temperature applications.

**Index Terms**—GaN, HEMT, micro-heater, WO<sub>3</sub>, NO<sub>2</sub> sensor.

## I. INTRODUCTION

RECENTLY, there have been growing concerns about environment pollution. The increasing demand for low power, compact, gas sensors for industrial and consumer applications drives the research of novel technologies towards miniaturization of the sensor without sacrificing sensitivity. Among polluting gases, nitrogen dioxide (NO<sub>2</sub>) is the one of the most harmful gases originating mainly from combustion of automobile exhaust (0.1~50 ppm) [1], furnaces, plants, etc. [2]

Manuscript received June 4, 2018; revised September 11, 2019; accepted September 17, 2019. Date of publication October 3, 2019; date of current version December 4, 2019. This work was supported by the Beijing Delft Institute of Intelligent Science and Technology. Subject Editor D. Devoe. (Corresponding authors: Pasqualina M. Sarro; Guoqi Zhang.)

J. Sun is with the Department of Microelectronics, Delft University of Technology, 2628 CD Delft, The Netherlands, and also with the China research Institute, Delft University of Technology, Beijing 100083, China (e-mail: sunjw15@163.com).

R. Sokolovskij is with the Department of Microelectronics, Delft University of Technology, 2628 CD Delft, The Netherlands, and with the Department of Electrical and Electronic Engineering, Southern University of Science and Technology, Shenzhen 518055, China, and also with the State Key Laboratory of Solid State Lighting, Changzhou 213161, China (e-mail: r.sokolovskij@tudelft.nl).

E. Iervolino, P. M. Sarro, and G. Zhang are with the Department of Microelectronics, Delft University of Technology, 2628 CD Delft, The Netherlands (e-mail: iervolino.elina@gmail.com; p.m.sarro@tudelft.nl; g.q.zhang@tudelft.nl).

Z. Liu is with the Institute of Microelectronic, Tsinghua University, Beijing 100084, China (e-mail: liuzw@tsinghua.edu.cn).

Color versions of one or more of the figures in this article are available online at <http://ieeexplore.ieee.org>.

Digital Object Identifier 10.1109/JMEMS.2019.2943403

The concentration varies quite heavily with different application environments, which creates the need for wearable, low power, continuous environmental monitoring systems. Current sensors are not suited for continuous air quality monitoring due to high power, slow response, and low sensitivity (ppb level). In this paper, a novel design of AlGaIn/GaN HEMT NO<sub>2</sub> gas sensor integrated with a micro-heater is presented. AlGaIn/GaN heterojunctions exhibit great potential for high performance sensors development due to high carrier density two-dimensional electron gas (2DEG) at the interface introduced by the strong polarization effect, which is sensitive to the changes in surface potential [3]. Compared to AlGaIn/GaN Schottky diode sensors for nitric oxide (NO)[2], ammonia (NH<sub>3</sub>) [4], [5], nitrogen dioxide (NO<sub>2</sub>) [6], hydrogen (H<sub>2</sub>) [7], and acetone [8], AlGaIn/GaN HEMT sensors provide several advantages: Firstly, the current to be measured is larger than that in Schottky diodes, resulting in higher current changes and lower theoretical detection limits. Secondly, the sensitivity can be modulated and optimized by changing the gate bias. Finally, the 2DEG does not interact with the analytes but is sensitive to surface states. By functionalizing the gate area of a HEMT sensor for different analytes, such as enzymes, polyimides, or metals, sensitivity to H<sub>2</sub> [7], NO<sub>2</sub> [9], NH<sub>3</sub> [9], [10], methane (CH<sub>4</sub>) [11], pH [12], urea [13], glucose [14], chloride ion [15], heavy metal [16], and DNA [17] have been reported.

As for most of chemical sensing, as shown in numerous experimental works and theoretical considerations, the important parameters such as selectivity, sensitivity, and response time of gas sensors can be improved by increasing the surface temperature. To sustain elevated operating temperature, a heating element is often integrated into the sensor system.

As shown in figure 1, a voltage or current controlled MEMS micro-heater, with a suspended and thus thermally isolated structure, enables low power heating. The micro-heater and HEMT sensor area were defined as active area. From previous work [18], a SiO<sub>2</sub> layer with low thermal conductivity provides an effective thermal isolation between the active sensor area and the silicon frame for substantial reduction of power consumption, down to 5-100 mW, when the active area of sensor is heated to the desired operating temperature.

Here, for the first time, we have fabricated suspended AlGaIn/GaN HEMT sensors with WO<sub>3</sub> nano-film modified gate and integrated MEMS microheater as a sensor platform. The sensor comprises an AlGaIn/GaN membrane suspended within a silicon frame micromachined out of the silicon

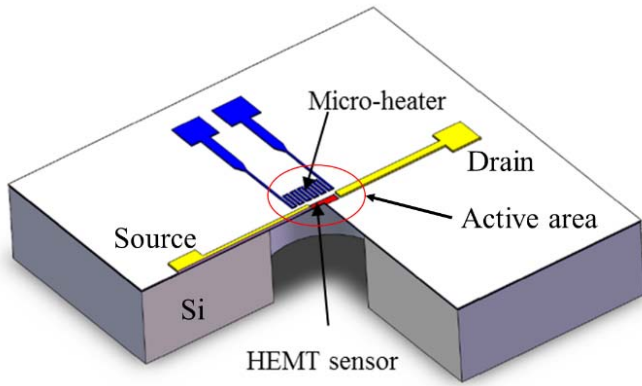


Fig. 1. Schematic of AlGaN/GaN HEMT integrated with micro-heater.

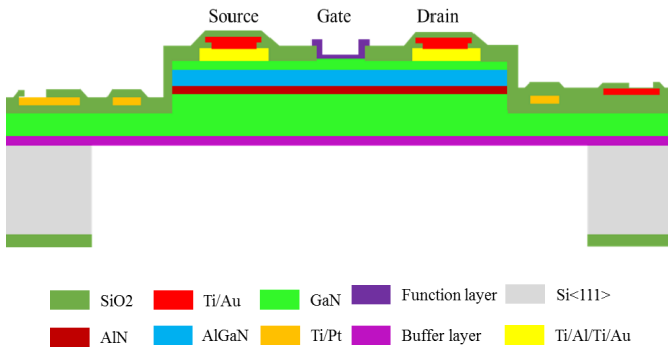


Fig. 2. Schematic cross-section of HEMT sensor structure.

wafer, and the following elements are over the membrane: a micro-heater which controls the temperature of the sensing layer, two  $\text{SiO}_2$  insulating layers, an HEMT sensor part and a  $\text{WO}_3$  nano-layer on top. The micro-heater performance and the AlGaN/GaN self-heating on the membrane structure are studied for the first time. In addition, the temperature and relative humidity effects on AlGaN/GaN sensor device are investigated and discussed. Finally, the response properties of HEMT sensor to  $\text{NO}_2$  gas with concentration of 0.1-40 ppm are presented. We conclude that the sensor concept that combines the HEMT sensor with a micro-heater can be applied to  $\text{NO}_2$  gases detection in consumer electronics and industrial applications.

## II. FUNDAMENTAL DESIGN AND FABRICATION PROCESSES

### A. Device Fabrication

Figure 2 presents a schematic drawing of the device cross-section. The HEMT sensor is placed together with the micro-heater surrounding the source/gate/drain area on a suspended membrane. The contact pads are on the thick silicon frame. The silicon substrate ( $400\ \mu\text{m}$ ) is backside etched away by deep reactive ion etching (DRIE) to form a circular membrane ( $650\ \mu\text{m}$  in diameter). The AlGaN/GaN heterostructure was grown by Suzhou Nanowin Co. on a 2-inch silicon  $\langle 111 \rangle$  1 mm-thick wafers using Metal-organic Chemical Vapor Deposition (MOCVD). Starting from the substrate structure consisted of, a  $2\ \mu\text{m}$ -thick undoped GaN buffer layer, followed

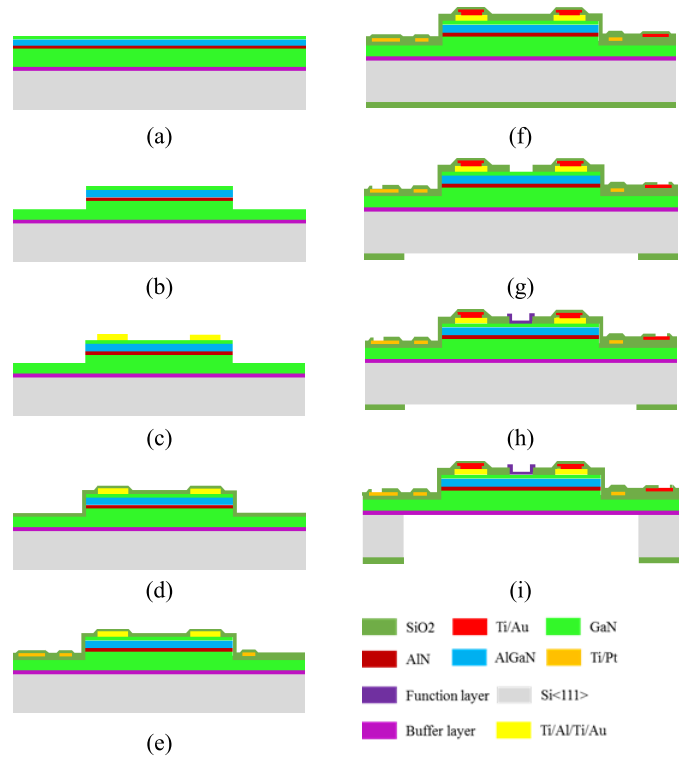


Fig. 3. Main steps for the fabrication of the suspended AlGaN/GaN HEMT sensor integrated with micro-heater. (a) starting wafer with epitaxial layers; (b) mesa etching to define sensor area; (c) Ohmic contact deposition and annealing; (d) PECVD  $\text{SiO}_2$ ; (e) micro-heater deposition and passivation; (f) metal deposition and top/bottom passivation; (g) opening contact pads at the frontside and etching window at the backside; (h) functional material deposition; (i) substrate etching from the backside to form the suspended structure.

by a 1 nm-thick AlN interlayer, an undoped 25 nm-thick  $\text{Al}_{0.26}\text{Ga}_{0.74}\text{N}$  barrier layer, and a 3 nm-thick GaN epitaxial cap layer. The electron mobility was  $\sim 1500\ \text{cm}^2/\text{V}\cdot\text{s}$ , with a sheet electron density of  $\sim 1 \times 10^{13}\ \text{cm}^{-2}$ .

The fabrication process flow (Fig.3) started with a mesa etching using a chlorine/boron chloride ( $\text{Cl}_2/\text{BCl}_3$ ) plasma to define the sensor geometry. Then, Ti/Al/Ti/Au (20/110/40/50 nm) metal contacts were e-beam evaporated and patterned by lift-off technology. Rapid thermal annealing at  $870^\circ\text{C}$  for 45 seconds under  $\text{N}_2$  ambient in a RTP-500 system was conducted to make the contacts Ohmic and improve reliability at high temperature. 200-nm Silicon dioxide ( $\text{SiO}_2$ ) was then deposited by plasma-enhanced chemical vapor deposition (PECVD). A Ti/Pt (30/200 nm) metal layer was deposited by e-beam evaporation and patterned by lift-off to form the micro-heater, followed by a 200-nm PECVD  $\text{SiO}_2$  layer for isolation from the interconnect layer. The  $\text{SiO}_2$  was patterned in buffer oxide etch (BOE) solution and the thick metal interconnect formed using evaporated a Ti/Au (20/300 nm) layer stack. The topside of the wafer was covered by PECVD  $\text{SiO}_2$  layer and the backside was polished down to  $400\ \mu\text{m}$  and  $5\ \mu\text{m}$ -thick  $\text{SiO}_2$  layer was deposited as hard mask during the DRIE process to etch the silicon substrate. Then backside  $\text{SiO}_2$  was patterned by inductively coupled plasma (ICP) etching using AZ4620 photoresist as mask and the topside  $\text{SiO}_2$  layer was etched in BOE solution to form opening for the contact pads

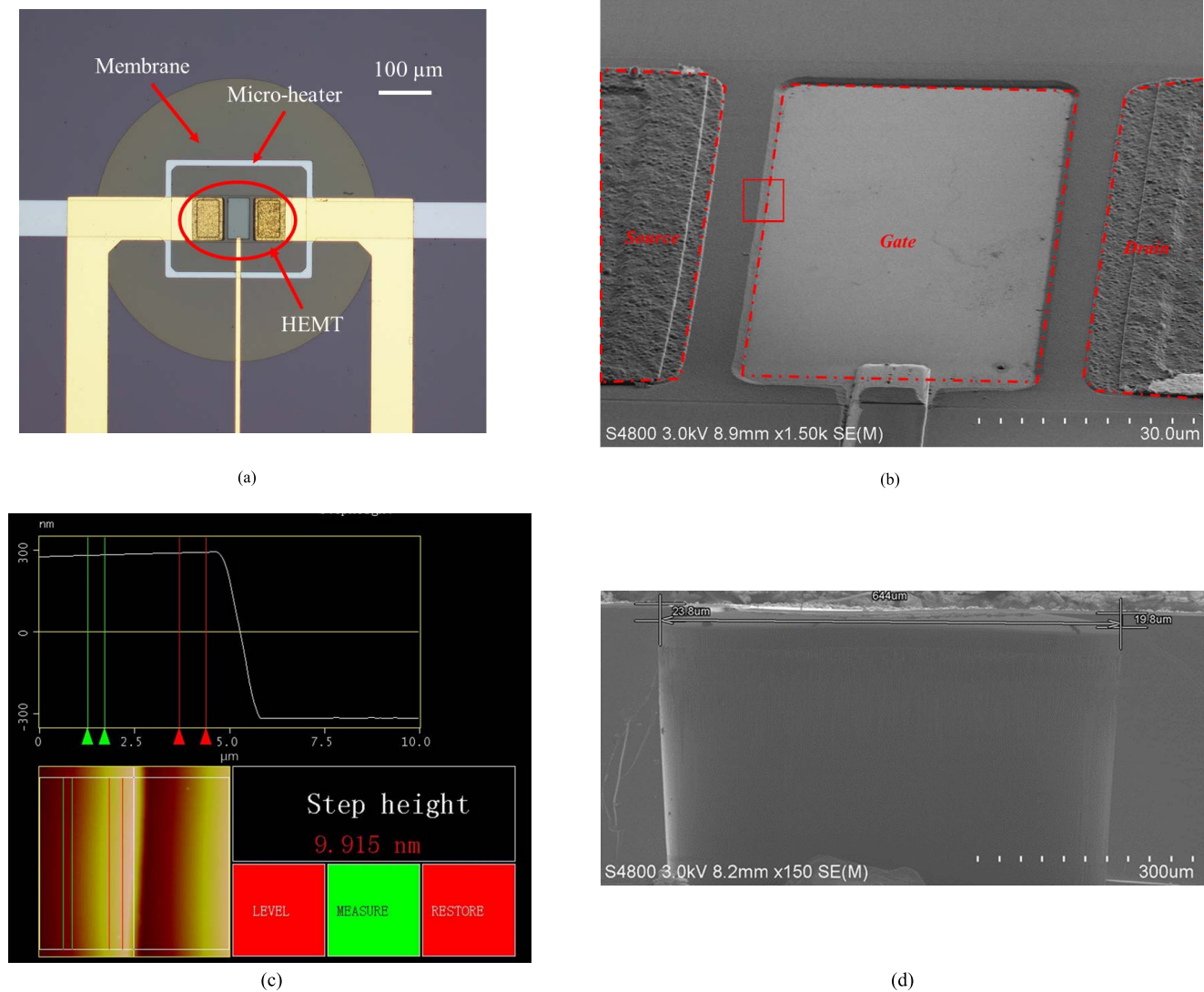


Fig. 4. The fabricated device: (a) optical image; (b) SEM image of HEMT sensor from 45° angle; (c) AFM image and step height measurement at red solid wireframe area of figure 4(b); (d) SEM image of the device cross section.

and gate windows. The WO<sub>3</sub> (10 nm) functional material layer was deposited on the gate area of 80 μm x 40 μm by physical vapor deposition (PVD). For comparison, the reference chip is without WO<sub>3</sub> layer deposition on gate area. The Silicon substrate is etched away below the active area in the final step. The microheater has a rectangle geometry around a central area of 230 μm x 290 μm, as showed in figure 4 (a). Figure 4 (b) and (d) show SEM images of the gate area from 45° angle and cross-sectional view of the fabricated sensor, respectively. Figure 4 (c) shows the AFM image and step height measurement of 10 nm WO<sub>3</sub> layer.

After dicing, the chips were wire-bonded to a prototype with ceramic quad flat no-lead (CQFN) package with size of 4 mm x 4 mm (Fig. 5). This sensor package is designed to eliminate the effect of gas flow by a perforated lid.

### B. Measurement Set Up

For gas testing experiments, the HEMT sensors were placed in a stainless steel chamber (20 mL) and connected to a

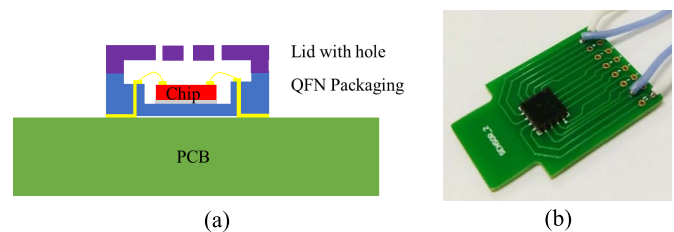


Fig. 5. (a) the schematic diagram of a gas sensor package; (b) the photograph of a packaged sensor on test PCB.

Keithley 2700 and a power source. Gas sources of pure N<sub>2</sub> and varying concentration of NO<sub>2</sub> were inserted in the testing chamber based on dynamic gas distribution instrument at atmospheric pressure. The gas flow rate was controlled at 100 sccm and the concentration of NO<sub>2</sub> in N<sub>2</sub> was varied from 100 ppb to 50 ppm at ambient temperature.

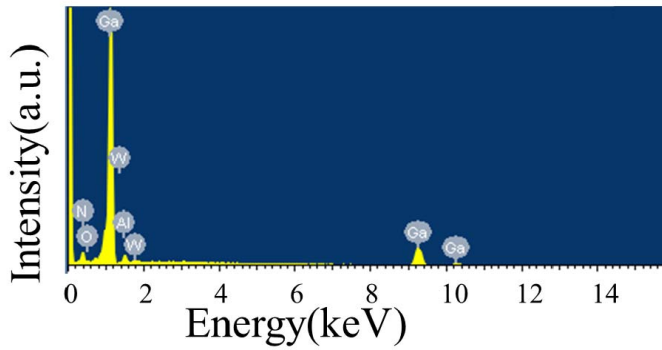


Fig. 6. EDS spectrum of the gate surface of the HEMT sensor.

### III. RESULTS AND DISCUSSION

The energy dispersive spectrum (EDS) of the device gate area surface is reported in figure 6. The corresponding peaks of Ga, W, N, Al, O elements are observed. Clearly, the deposition of  $\text{WO}_3$  on the gate surface by magnetron sputtering is confirmed.

#### A. Micro-Heater Calibration and Thermal Characterization

Before the heater is used as heating element, it is necessary to perform a calibration for extracting the temperature of active area, which is between source and gate. The sample is placed in an oven and the temperature was varied from 303.15 K up to 353.15 K and the resistance versus temperature curve has been recorded. Low current values are supplied to the Pt heater element to prevent self-heating of the heater itself. The temperature dependence of the resistivity is well described by the following linear equation:

$$\rho_H(T) = \rho_0 [1 + \alpha (T - T_0)] \quad (1)$$

where  $\rho_H$  and  $\rho_0$  are, respectively, the heater resistivity at temperature  $T$  and at ambient temperature  $T_0$ ;  $\alpha$  is the thermal coefficient of resistance (TCR). The measured TCR of the heater is equal to 3861 ppm/K with a deviation of 10 ppm/K according to the RTD standard [19].

However, the self-heating effect of the AlGaN/GaN HEMT device also causes a local increase in crystal temperature due to the dissipated Joule electric power. The combined thermal characteristic of the Pt micro-heater and the HEMT self-heating at ambient temperature is shown in Figure 7. The surface temperature can be measured by infrared radiation (IR) thermal camera or extracted by the resistance change of the micro-heater at ambient temperature, showing a linear growth with increasing the drain-source voltage,  $V_{DS}$ . Figure 7 shows the max temperature distribution on the gate surface when changing the voltage of drain-source,  $V_{DS}$ , and micro-heater,  $V_H$ . Figure 8 shows measured heating power consumption of micro-heater and temperature versus microheater voltage at  $V_{DS} = 5$  V. As adding the voltage of micro-heater,  $V_H$ , the max temperature of gate surface will nonlinear grow. When the voltage of micro-heater is  $V_H = 4$  V and  $V_H = 3$  V, the max gate surface temperature is about 297.87 °C and 135 °C. In fact, the power of sensor is about 200 mW when the

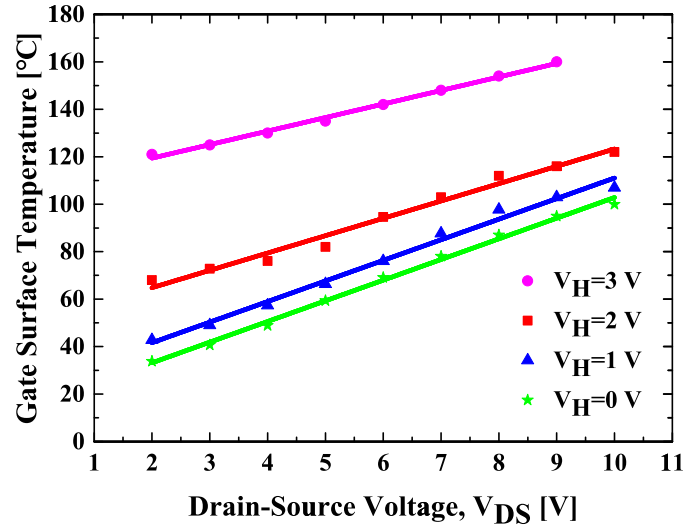


Fig. 7. Combined heating characteristic of the Pt micro-heater and HEMT self-heating at ambient temperature of 298.15 K for voltage of micro-heater,  $V_H = 0$  V to 3 V and  $V_{DS} = 2$  V to 10 V with 1 V increments.

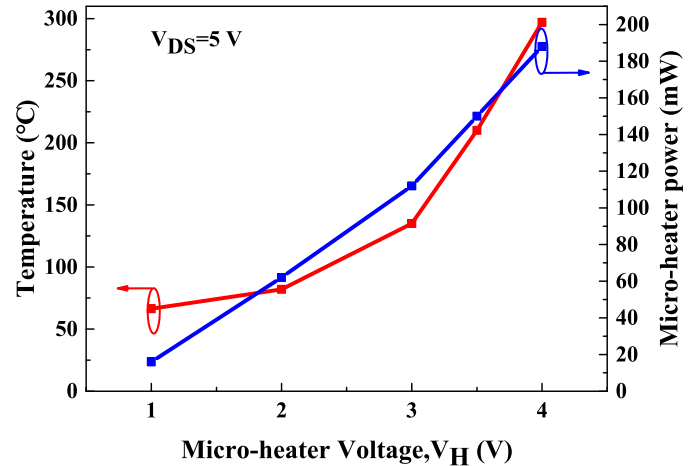


Fig. 8. Measured heating power consumption of micro-heater and temperature versus microheater voltage at  $V_{DS} = 5$  V.

operating temperature is about 300 °C. The reasons of a little high power maybe as following: one is the residual Si around the membrane during the DRIE process; another one is the ceramic package with high thermal conductivity coefficient resulting in increased the power consumption. The power of the sensor will be optimized in the next phase. To further improve heating efficiency, a larger size membrane and cycle heating [10] can be utilized.

#### B. Temperature and Humidity Measurement

The AlGaN/GaN HEMT devices were tested versus ambient temperature and humidity in the 263 K to 353 K range, with 10 K steps, and the 5% RH to 90% RH range. The gate voltage of the HEMT device was left floating and  $V_{DS}$  varied from 0V to 20 V. As shown in figure 9, the saturated current has a little drop with raising  $V_{DS}$  due to the thermal and lattice scattering of the 2DEG. And the  $I_{DS}$  decreases remarkably between 263 K and 353 K at 20% RH. The saturated current

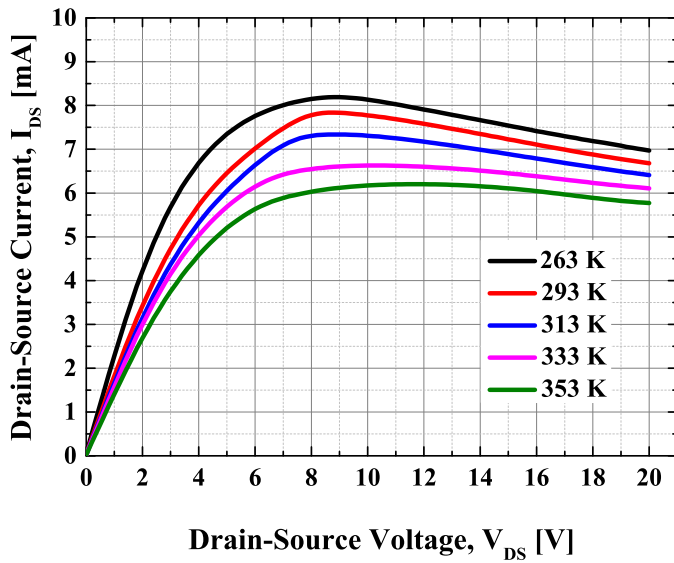


Fig. 9. I-V characteristics of HEMT sensor under variable ambient temperature at 20% relative humidity.

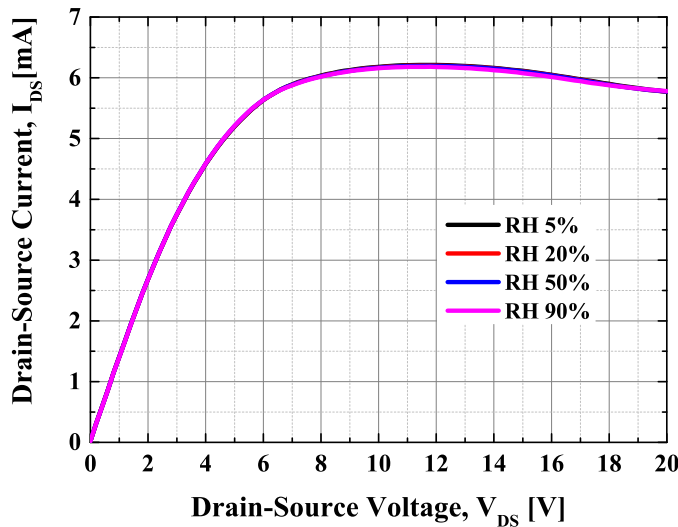


Fig. 10. I-V characteristics of HEMT sensor under different relative humidity at 353.15 K.

temperature coefficient is  $-0.63 \text{ mA/mm}\cdot\text{K}$ , which is in agreement with results from literature [20]. Figure 10 indicates that the relative humidity has no significant effect on the I-V characteristics of HEMT at 353.15 K. The humidity effect at different temperatures is shown in Figure 11. The  $I_{DS}$  decreases upon increasing the relative humidity from 5% to 90% at low temperature. However, the effect of relative humidity on  $I_{DS}$  becomes insignificant with increasing ambient temperature. Of course, the temperature influence should be avoided during measurement. In order to eliminate the temperature interference, a differential method (including a second structure with the same geometry but not exposed to gas/humidity in one chip) can be a suitable solution.

### C. Gas Sensing Measurement

The gas sensors were placed in the testing chamber and heated to 571 K while exposed to 0.1-40 ppm NO<sub>2</sub>

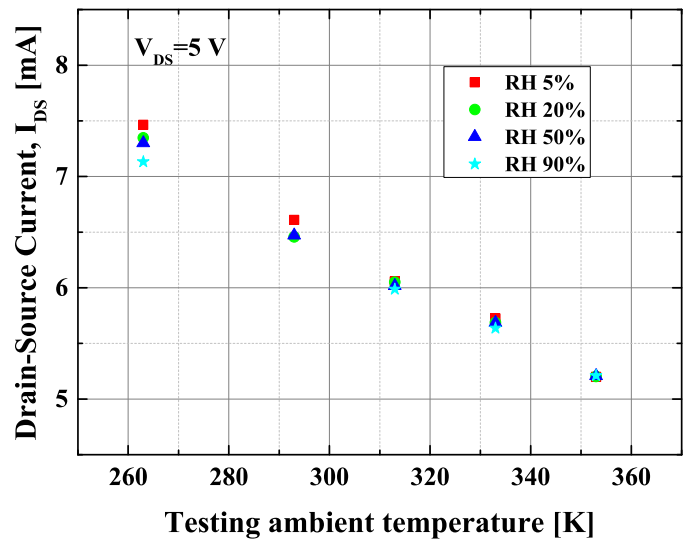


Fig. 11. Temperature and relative humidity effect on the  $I_{DS}$  of HEMT sensor at  $V_{DS} = 5 \text{ V}$ .

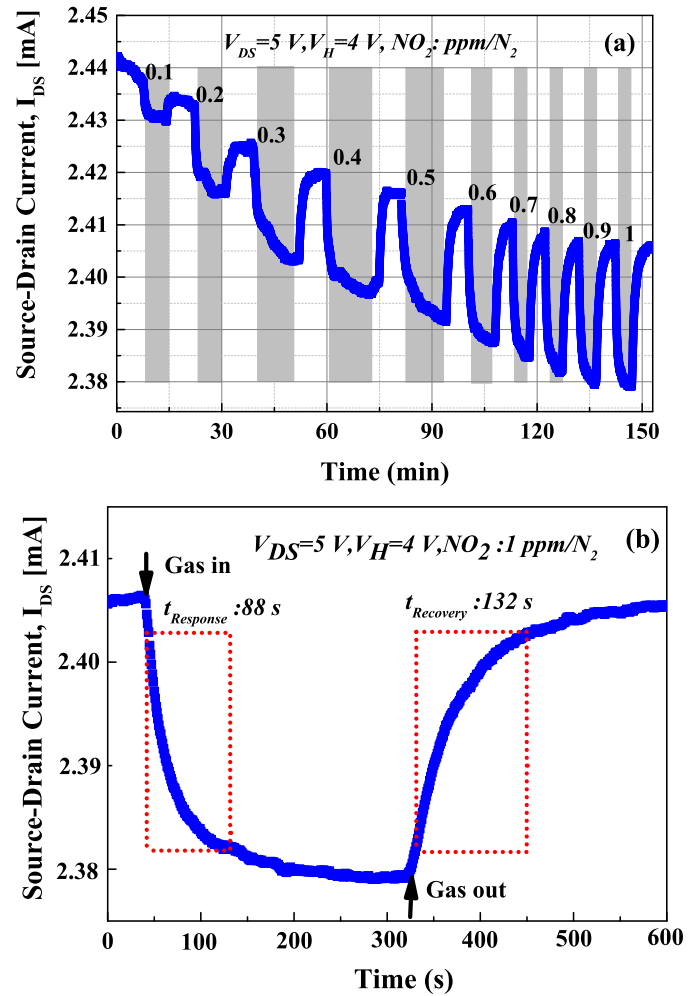


Fig. 12. Transient response of AlGaIn/GaN HEMT sensor to NO<sub>2</sub> gas concentrations at  $\sim 300 \text{ }^\circ\text{C}$  (a) 0.1-1 ppm. (b) Enlarged part of the response curve of 1 ppm.

gas in pure N<sub>2</sub>. Figure 12 (a) presents that the transient response of AlGaIn/GaN sensor for 0.1-1 ppm at the operating bias of  $V_{DS} = 5 \text{ V}$  and  $V_H = 4 \text{ V}$ . A clear effect is

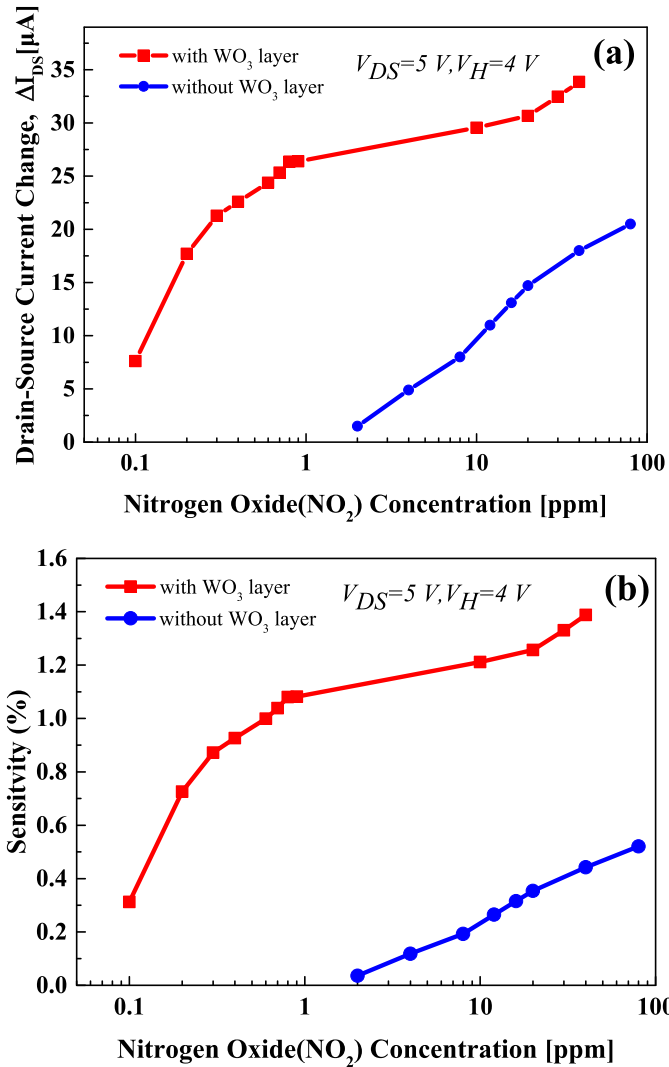


Fig. 13. Gas concentration dependent sensing properties of HEMT sensor for 0.1-80 ppm NO<sub>2</sub> gas at ~300 °C.

observed under a low concentration of 100 ppb NO<sub>2</sub>/N<sub>2</sub> at ~ 300 °. Figure 12 (b) shows the enlarged parts of data in figure 12 (a) measured at a NO<sub>2</sub> concentration of 1 ppm. To qualify a sensor to be efficient, response time and recovery time are crucial to be determined. Response time ( $t_{\text{Response}}$ ) and recovery time ( $t_{\text{Recovery}}$ ) were defined as the time required for the drain current to change/return from 10% to 90 % of its saturated response value to NO<sub>2</sub> gas. And as shown in Figure 13, the current change values ( $\Delta I$ ) and sensitivity ( $S = \Delta I/I$ ) toward NO<sub>2</sub> gas increase after WO<sub>3</sub> layer deposition. At the concentration of 10 ppm,  $\Delta I$  and  $S$  were found to increase from 9 μA and 0.25% to 29 μA and 1.21%, respectively. And the limit of sensor detection also be improved from 2 ppm to 100 ppb. Figure 14 characterizes the response time and recovery time as function of NO<sub>2</sub> concentration with WO<sub>3</sub> layer and without WO<sub>3</sub> layer. The response time of sensor with WO<sub>3</sub> layer is improved from 423 second to 91 second at 10 ppm. However, the recovery time of device without WO<sub>3</sub> layer are faster. The possible reason is that the AlGaIn surface is easy for NO<sub>2</sub> molecule desorption. At the concentration

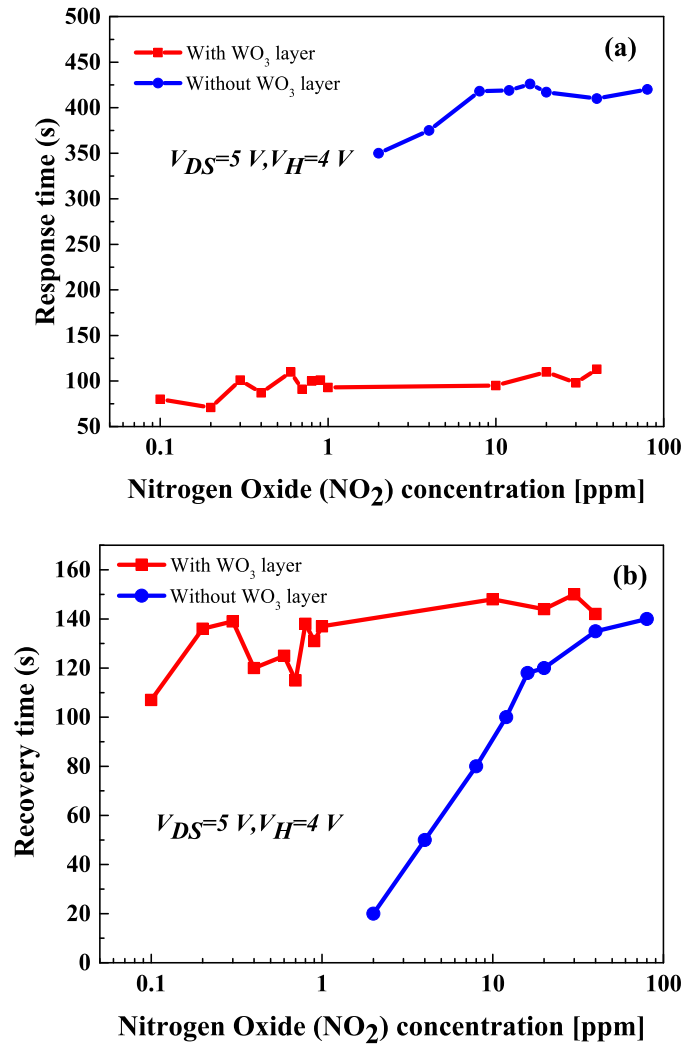


Fig. 14. Response time (b) and recovery time (c) versus NO<sub>2</sub> concentration.

of 1 ppm,  $\Delta I$  and  $S$  were found to be 26 μA and 1.1% with a response and recovery time of 88 second and 132 second, respectively. The response times could be further reduced with a shorter distance between the gas cylinder and the sensor. The effect of the working temperature, known to have great influence on the sensitivity of gas sensor, was studied as well. The current change and sensitivity as a function of micro-heater voltage are plotted in Figure 15. The sensitivity of sensor exposed to 10 ppm NO<sub>2</sub> at  $V_H = 3\text{ V}$  (135 °),  $V_H = 3.5\text{ V}$  (210 °) and  $V_H = 4\text{ V}$  (300 °) are 0.29%, 0.9% and 1.4 %, respectively. The sensing properties are significantly enhanced with increasing micro-heater voltage (temperature). Nano WO<sub>3</sub> gate AlGaIn/GaN HEMT sensors have shown a great potential to detect low NO<sub>2</sub> concentration with a fast response time.

#### D. Sensing Mechanism

Several potential sensing mechanisms have been reported based on adsorption on surface of catalytic metal dissociate and release electrons [9], [21], [22] When the sensor are exposed to NO<sub>2</sub> gas, chemisorption reaction on the WO<sub>3</sub>



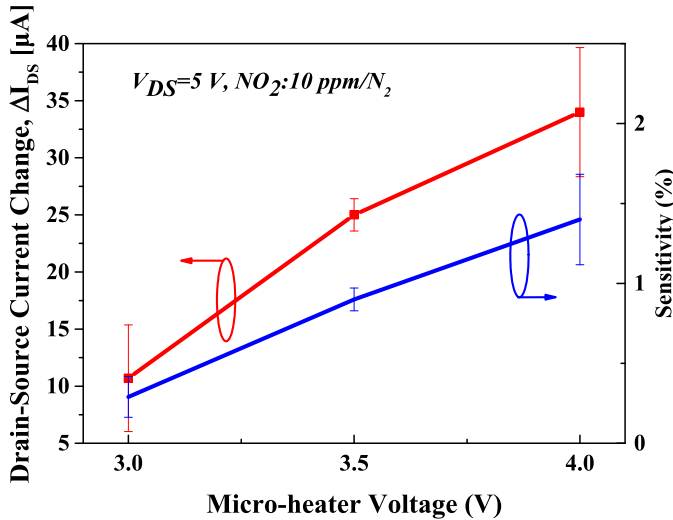
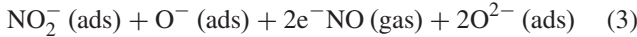
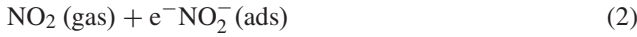


Fig. 15. Current change and sensitivity of sensor with WO<sub>3</sub> layer to 10 ppm NO<sub>2</sub> at different micro-heater voltages (temperature).

surface results in gas ions (negatively charged for NO<sub>2</sub>) that rapidly diffuse at the surface. NO<sub>2</sub> gas adsorb directly on the surface of WO<sub>3</sub> layer as well as reacts with adsorbed O<sup>-</sup> ions according to the following reaction [23]



On the other hand, the surface states would be altered by the polar NO<sub>2</sub> molecules, which would manipulate the 2DEG concentration. Therefore, the surface potential of the WO<sub>3</sub> and AlGaIn are changed, resulting in the variation of drain current of the HEMT device. The changed surface potential can mathematically be represented by the Helmholtz model

$$\Delta V = \frac{N_S p (\cos\theta)}{\epsilon \epsilon_0} \quad (4)$$

where  $p$  is the dipole moment,  $N_S$  is the dipole density per unit area,  $\theta$  is the angle between the dipole and the normal surface,  $\epsilon$  is the relative permittivity of the material, and  $\epsilon_0$  is the permittivity of free space. The surface potential is major affected by the value of  $p/\epsilon$  of the polar molecules.

#### IV. CONCLUSIONS

In conclusion, nano-film WO<sub>3</sub> gate AlGaIn/GaN HEMT sensors integrated with micro-heater on suspended membrane have been microfabricated and characterized. The combined effect of micro-heater heating and self-heating on membrane has been studied first time. Significant detection is observed under a low concentration of 100 ppb NO<sub>2</sub>/N<sub>2</sub> at ~300 °. As exposed to a 1 ppm NO<sub>2</sub> gas, a high sensing sensitivity of 1.1% with a response (recovery) time of 88 second (132 second) is obtained. The sensor shows is not affected under high relative humidity ambient while the temperature influence need be avoided. Based on the excellent sensing performance and inherent advantages of low power consumption, the HEMT

sensor combined nano-film WO<sub>3</sub> functional gate and micro-heater provides an attractive alternative for high performance NO<sub>2</sub> sensing applications.

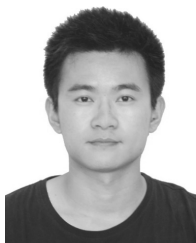
#### ACKNOWLEDGMENT

Fabio Santagata is acknowledged for his kind help during the design and processes. The authors would like to thank Prof. Junxi Wang and the staff of the Institute of Semiconductor, Chinese Academy of Sciences for their assistance in device fabrication, and Xueping Guo from Institute of Microelectronic of Chinese Academy of Sciences for the packaging.

#### REFERENCES

- [1] M. A. Chougule, S. Sen, and V. B. Patil, "Fabrication of nanostructured ZnO thin film sensor for NO<sub>2</sub> monitoring," *Ceram. Int.*, vol. 38, no. 4, pp. 2685–2692, May 2012.
- [2] V. Tilak, K. Matocha, and P. Sandvik, "Pt/GaN Schottky diodes for harsh environment NO sensing applications," *Phys. Status Solidi c*, vol. 2, no. 7, pp. 2555–2558, May 2005.
- [3] O. Ambacher, J. Smart, J. R. Shealy, N. G. Weimann, K. Chu, M. Murphy, W. J. Schaff, and L. F. Eastman, "Two-dimensional electron gases induced by spontaneous and piezoelectric polarization charges in N- and Ga-face AlGaIn/GaN heterostructures," *J. Appl. Phys.*, vol. 85, no. 6, pp. 3222–3233, Mar. 1999.
- [4] T.-Y. Chen *et al.*, "Ammonia sensing properties of a Pt/AlGaIn/GaN Schottky diode," *IEEE Trans. Electron Devices*, vol. 58, no. 5, pp. 1541–1547, May 2011.
- [5] P. C. Chou *et al.*, "Study of an electroless plating (EP)-based Pt/AlGaIn/GaN Schottky diode-type ammonia sensor," *Sens. Actuators B, Chem.*, vol. 203, pp. 258–262, Nov. 2014.
- [6] J. Schalwig, G. Muller, M. Eickhoff, O. Ambacher, and M. Stutzmann, "Group III-nitride-based gas sensors for combustion monitoring," *Mater. Sci. Eng. B-Solid State Mater. Adv. Technol.*, vol. 93, nos. 1–3, pp. 207–214, May 30 2002.
- [7] S. Jang, P. Son, J. Kim, S.-N. Lee, and K. H. Baik, "Hydrogen sensitive Schottky diode using semipolar (1122) AlGaIn/GaN heterostructures," *Sens. Actuators B, Chem.*, vol. 222, pp. 43–47, Jan. 2016.
- [8] S. Das, S. Majumdar, R. Kumar, S. Ghosh, and D. Biswas, "Thermodynamic analysis of acetone sensing in Pd/AlGaIn/GaN heterostructure Schottky diodes at low temperatures," *Scripta Mater.*, vol. 113, pp. 39–42, Mar. 2016.
- [9] C. Bishop *et al.*, "Experimental study and device design of NO, NO<sub>2</sub>, and NH<sub>3</sub> gas detection for a wide dynamic and large temperature range using Pt/AlGaIn/GaN HEMT," *IEEE Sensors J.*, vol. 16, no. 18, pp. 6828–6838, Sep. 2016.
- [10] P. Offermans *et al.*, "Suspended AlGaIn/GaN membrane devices with recessed open gate areas for ultra-low-power air quality monitoring," in *IEDM Tech. Dig.*, Dec. 2015, pp. 33.6.1–33.6.4.
- [11] Y. Y. Xi, L. Liu, and F. Ren, "Methane detection using Pt-gated AlGaIn/GaN high electron mobility transistor based Schottky diodes," *J. Vac. Sci. Technol. B*, vol. 31, no. 3, May 2013, Art. no. 032203.
- [12] M. S. Z. Abidin, A. M. Hashim, M. E. Sharifabad, S. F. Rahman, and T. Sadoh, "Open-gated pH sensor fabricated on an undoped-AlGaIn/GaN HEMT structure," *Sensors*, vol. 11, no. 3, pp. 77–3067, Mar. 2011.
- [13] C.-T. Lee and Y.-S. Chiu, "Gate-recessed AlGaIn/GaN ISFET urea biosensor fabricated by photoelectrochemical method," *IEEE Sensors J.*, vol. 16, no. 6, pp. 1518–1523, Mar. 2016.
- [14] B. H. Chu *et al.*, "Aluminum gallium nitride (GaN)/GaN high electron mobility transistor-based sensors for glucose detection in exhaled breath condensate," *J. Diabetes Sci. Technol.*, vol. 4, no. 1, pp. 9–171, Jan. 2010.
- [15] B.-H. Chu *et al.*, "Chloride ion detection by InN gated AlGaIn/GaN high electron mobility transistors," *J. Vac. Sci. Technol. B, Microelectron.*, vol. 28, no. 1, pp. L5–L8, Jan. 2010.
- [16] J. Cheng *et al.*, "Ultrasensitive detection of Hg<sup>2+</sup> using oligonucleotide-functionalized AlGaIn/GaN high electron mobility transistor," *Appl. Phys. Lett.*, vol. 105, no. 8, Aug. 2014, Art. no. 083121.
- [17] N. Espinosa, S. U. Schwarz, V. Cimalla, and O. Ambacher, "Detection of different target-DNA concentrations with highly sensitive AlGaIn/GaN high electron mobility transistors," *Sens. Actuators B, Chem.*, vol. 210, pp. 633–639, Apr. 2015.

- [18] J. Lee *et al.*, "Low power consumption solid electrochemical-type micro CO<sub>2</sub> gas sensor," *Sens. Actuators B, Chem.*, vol. 248, pp. 957–960, Sep. 2017.
- [19] J. Li and G. Peterson, "Microscale heterogeneous boiling on smooth surfaces—From bubble nucleation to bubble dynamics," *Int. J. Heat Mass Transfer*, vol. 48, nos. 21–22, pp. 4316–4332, 2005.
- [20] Y. Halfaya *et al.*, "Investigation of the performance of HEMT-based NO, NO<sub>2</sub> and NH<sub>3</sub> exhaust gas sensors for automotive antipollution systems," *Sensors*, vol. 16, no. 3, p. 273, Feb. 2016.
- [21] T.-Y. Chen *et al.*, "On an ammonia gas sensor based on a Pt/AlGaN heterostructure field-effect transistor," *IEEE Electron Device Lett.*, vol. 33, no. 4, pp. 612–614, Apr. 2012.
- [22] B. Urasinska-Wojcik, T. A. Vincent, M. F. Chowdhury, and J. W. Gardner, "Ultrasensitive WO<sub>3</sub> gas sensors for NO<sub>2</sub>, detection in air and low oxygen environment," *Sens. Actuators B, Chem.*, vol. 239, pp. 1051–1059, Feb. 2017.
- [23] S. Park, H. Ko, S. Kim, and C. Lee, "Gas sensing properties of multiple networked GaN/WO<sub>3</sub> core-shell nanowire sensors," *Ceram. Int.*, vol. 40, no. 6, pp. 8305–8310, Jul. 2014.



**Jianwen Sun** received the M.S. degree in microelectronics from Tsinghua University in 2015. He is currently pursuing the Ph.D. degree in electrical engineering with the Delft University of Technology, Delft, The Netherlands. His current research interests include design, fabrication and characterization of wide bandgap gallium nitride (GaN)-based UV, and chemical sensors.



**Robert Sokolovskij** received the B.S. degree in electronics engineering from Vilnius University, Vilnius, Lithuania, in 2010, and the M.S. degree in electrical engineering from the Delft University of Technology, Delft, The Netherlands, in 2013, where he is currently pursuing the Ph.D. degree. Since 2014, he has been with the State Key Laboratory of Solid State Lighting, Changzhou, China. Since 2018, he has been a part-time Research Assistant with the Southern University of Science and Technology, Shenzhen, China. His current research interests

include design, fabrication, and characterization of wide bandgap gallium nitride (GaN)-based power electronic devices, and chemical sensors.



**Elina Iervolino** received the Ph.D. degree in MEMS system from the Delft University of Technology in 2012. She is currently a Post-Doctoral Researcher with Peking University, China. Her research interests include novel sensor development for environmental and healthcare applications.



Electronics and the Chinese Society of Micro/Nanotechnology.

**Zewen Liu** received the B.S. degree in physics from the University of Science and Technology of China, Hefei, China, in 1983, and the Ph.D. degree in instrument physics from the University of Paris-Sud, Paris, France. From 1983 to 1993, he was with the Hefei National Synchrotron Radiation Laboratory. Since 1993, he has been with Tsinghua University, Beijing, China, where he is currently with the Institute of Microelectronics, and also involved in novel IC devices and microsystem technologies. He is a Senior Member of the Chinese Institute of



**Pasqualina M. Sarro** (F'06) received the Laurea degree (*cum laude*) in solid-states physics from the University of Naples, Italy, in 1980, and the Ph.D. degree in electrical engineering from the Delft University of Technology, The Netherlands, in 1987. From 1981 to 1983, she was a Post-Doctoral Fellow with the Division of Engineering, Photovoltaic Research Group, Brown University, Providence, RI, USA. Since then, she has been with the Delft Institute of Microsystems and Nanoelectronics, Delft University of Technology, where she has been

responsible for research on integrated silicon sensors and MEMS technology. In 2001, she became an A. van Leeuwenhoek Professor. Since 2004, she has been the Head of the Electronic Components, Materials, and Technology Laboratory. Since 2009, she has been the Chair of the Microelectronics Department, Delft University. She has authored or coauthored over 400 journals and conference articles. In 2006, she became a member of the Royal Netherlands Academy of Arts and Sciences. She is a member of the Technical Program Committee and the International Steering Committee for several international conferences, including the IEEE MEMS, the IEEE Sensors, Eurosensors, and Transducers. In 2006, she was elected as an IEEE Fellow for her contribution to micromachined sensors, actuators, and microsystems. In 2004, she was a recipient of the EUROSENSORS Fellow Award for her contribution to the field of sensor technology. She is also the Technical Program Co-Chair of the First IEEE Sensors 2002 Conference and the Technical Program Chair of the Second and the Third IEEE Sensors Conference in 2003 and 2004 and the General Co-Chair of the IEEE MEMS 2009. She will act as the General Co-Chair for the IEEE Sensors 2014 and the European TPC Chair for Transducers 2015.



**Guoqi Zhang** received the Ph.D. degree in aerospace engineering from the Delft University of Technology, Delft, The Netherlands, in 1993. He was with Philips for 20 years as the Principal Scientist, from 1994 to 1996, the Technology Domain Manager, from 1996 to 2005, the Senior Director of the Technology Strategy, from 2005 to 2009, and a Philips Fellow, from 2009 to 2013. He also had part-time appointments as a Professor with the Technical University of Eindhoven, from 2002 to 2005, and the Chair Professor with the Delft University of

Technology, from 2005 to 2013, where he has been the Chair Professor with the Department of Microelectronics, since 2013. As one of the renowned players in the fields of semiconductors and SSL technologies, he is also the Deputy Director of the European Center for Micro- and Nanoreliability (EUCEMAN), the Vice Chairman of the Chinese Electronics Packaging Association, and the China Co-Chairman of the Advisory Board of International Solid State Lighting Alliance (ISA). His current research interests include micro/nanoelectronics system integration, microsystems packaging, and assembly technologies and reliability.